Turkish Journal of Chemistry

http://journals.tubitak.gov.tr/chem/

Research Article

Turk J Chem
(2019) 43: 1350 – 1364

doi:10.3906/kim-1904-57

# Natural diterpenoid alysine A isolated from *Teucrium alyssifolium* exerts antidiabetic effect via enhanced glucose uptake and suppressed glucose absorption

**Alaattin ŞEN**[1,2,*], **Buket AYAR**[1], **Anıl YILMAZ**[3], **Özden Özgün ACAR**[1], **Gurbet Çelik TURGUT**[1], **Gülaçtı TOPÇU**[3]

[1]Department of Biology, Faculty of Arts and Sciences, Pamukkale University, Denizli, Turkey
[2]Department of Molecular Biology and Genetics, Faculty of Life Sciences, Abdullah Gül University, Kayseri, Turkey
[3]Department of Pharmacognosy and Phytochemistry, Faculty of Pharmacy, Bezmialem Vakıf University, İstanbul, Turkey

**Received:** 29.04.2019 • **Accepted/Published Online:** 29.07.2019 • **Final Version:** 07.10.2019

**Abstract:** *Teucrium* species have been used in folk medicine as antidiabetic, antiinflammatory, antiulcer, and antibacterial agents. We have explored in vitro antidiabetic impacts of 2 natural diterpenoids, alysine A and alysine B, isolated from *Teucrium alyssifolium*. The lactate dehydrogenase (LDH) cytotoxicity assay, glucose uptake test, glucose utilization (glycogen content) test, glucose transport test, glucose absorption ($\alpha$-glucosidase activity) test, insulin secretion test, RNA isolation and cDNA synthesis assay, qPCR quantification assays, and statistical analyses were carried out in the present study. Alysine A exerted the following effects at non-cytotoxic doses:

- Enhanced the glucose uptake, as much as the insulin in the C2C12, HepG2, and 3T3-L1 cells
- Increased the glycogen content in the C2C12 and HepG2 liver cells, significantly higher than the insulin and metformin
- Suppressed the alpha-glucosidase and the GLUT2 expression levels in the Caco-2 cells
- Suppressed the SGLT1 and GLUT1-5 expression levels in the Caco-2 cells
- Induced the insulin receptor substrate (IRS)1 and GLUT2 expression levels of the BTC6 pancreatic cells
- Induced the insulin receptor (INSR), IRS2, phosphoinositide 3-kinase (PI3K), GLUT4, and protein kinase (PK) expression levels of the 3T3-L1 and C2C12 cells
- Increased glucose transport through the Caco-2 cell layer
- Did not influence insulin secretion in the pancreatic BTC6 cells

Consequently, these data strongly emphasized the antidiabetic action of alysine A on the particularly critical model mechanisms that assume a part in glucose homeostasis, such as glucose uptake, utilization, and storage. Moreover, the expression level of the essential genes in glucose metabolism and insulin signaling was altered in a way that the results would be antihyperglycemic. A blend of in vitro and in situ tests affirmed the antihyperglycemic action of alysine A and its mechanism. Alysine A has exercised significant and positive results on the glucose homeostasis; thus, it is a natural and pleiotropic antidiabetic agent. Advanced in vivo studies are required to clarify the impact of this compound on glucose homeostasis completely.

**Key words:** Alysine A, alysine B, antidiabetic, *Teucrium alyssifolium,* glucose homeostasis

*Correspondence: sena@agu.edu.tr

## 1. Introduction

The genus *Teucrium*, a member of the family Lamiaceae, has approximately 300 species worldwide, mostly in the Mediterranean region. *Teucrium* is represented by 46 taxa in Turkey, 16 of which are endemic. *Teucrium* species have been used in folk medicine as antidiabetic, antiinflammatory, antiulcer, and antibacterial agents [1]. Studies have shown that *Teucrium* species demonstrate antimicrobial, antioxidant, and antifungal activities [2]. The main compounds isolated from *Teucrium* species to date are clerodane and neoclerodane diterpenes [3]. Therefore, it can be opined that clerodane and neoclerodane diterpenoids could be responsible for those activities that *Teucrium* species exhibit. For this reason, these precious natural diterpenes were obtained by isolating or synthesizing.

Diabetes mellitus (DM) is a chronic disease that occurs when the insulin hormone that regulates blood sugar is not sufficiently produced or when the body cannot use insulin efficiently. Hyperglycemia, or high blood sugar, that occurs when DM is not controlled, leads to severe damage over time, especially in many systems of the body, such as nerves and blood vessels. It has been reported that 347 million people worldwide have diabetes [4]. In 2004, about 3.4 million people were reported to have died as a result of high blood sugar [5] and similar figures for 2010 are estimated. Reflection and estimation studies predict that diabetes will be the seventh largest cause of death in the world by 2030 [5].

The most common form of diabetes is type 2 DM (T2DM), although there are 3 major forms of diabetes. In T2DM patients, cells do not respond appropriately to insulin (insulin resistance), resulting in glucose storage deficiency. Insulin resistance can develop in later ages, especially with long-term high-calorie diets and other risk factors. Insulin resistance causes a disorder of the complex signaling mechanism between adipose tissue, pancreatic islets, liver, and skeletal muscle [6–8]. The specific molecular pathology of the disease is not evident; family history, changes in early development, excessive nutrient intake, obesity, lack of physical activity, and aging pave the way for disease development. Mitochondrial oxidative metabolism and adenosine triphosphate production, fatty acid oxidation, proinflammatory signaling, and a change in the development and metabolism of beta cells can reduce insulin secretion. This can lead to insulin resistance as it impairs insulin signaling [9].

The use of medicinal herbs for the treatment of diabetes extends back to the Ebers Papyrus of 1550 BC [10]. Despite the discovery and use of insulin and other modern oral hypoglycemic agents, the search for safer and more efficacious herbal medicines for the treatment of diabetes continues [10]. Because of the high cost of insulin and lack of medical care, many herbal uses remain an alternative, especially in poor communities. *Teucrium* species are characterized as a hypoglycemic adjunct without any detailed and precise knowledge of the mode of action, without any adverse effects for years on T2DM, especially *T. polium* [11,12]. With the extract of *Teucrium alyssifolium* Stapf, which is endemic to Turkey, its antidiabetic effect was detected during our pilot screening study in the laboratory. This data suggested the potential antidiabetic effect of *T. alyssifolium*.

Secondary metabolites acquired from plants, particularly those utilized traditionally, are at the pioneers of new medicine development in fighting diseases like diabetes. It is known that isolated or synthesized terpenoids have shown an antidiabetic effect [13–18], as well as antioxidant, anticholinesterase, and opioid receptor activities [19–21]. In this context, the antihyperglycemic activity of 2 pure diterpenoid compounds, alysine A and alysine B, previously isolated from *T. alyssifolium*, an endemic species of *Teucrium*, was first investigated by in vitro models.

## 2. Materials and methods

### 2.1. Materials

The following were used in this study: dimethylbiguanide hydrochloride, 3-Isobutyl-1-methylxanthine, 96-well microplates, (D - (+) - glucose, dexamethasone, dimethyl sulfoxide (DMSO), calcium chloride, L-glutamine, maltose solution, bovine serum albumin (BSA), insulin solution, and sucrose (Sigma-Aldrich, St. Louis, MO, USA); EasyScript™plus cDNA synthesis kit and KiloGreen 2X qPCR (MasterMix-KS) (Applied Biological Materials Inc., BC, Canada); 3T3-L1, C2C12, HepG2, and BTC6 cell lines (LGS Standards GmbH, Wesel, Germany); For the primers, 50 nmol of Oligo-DNA (GenScript, NJ, USA); Gibco fetal bovine serum (FBS) (Thermo Fisher Scientific, MA, USA); Dulbecco's modified Eagle's medium (DMEM), Dulbecco's phosphate buffered saline (PBS), Eagle's modified essential medium (EMEM), penicillin-streptomycin mixture, and trypsin-ethylenediaminetetraacetic acid (EDTA) solution (Lonza Group Ltd., Basel, Switzerland); insulin enzyme-linked immunosorbent assay (ELISA) kit (EMD Millipore Corp., MA, USA); RNeasy plus mini kit (74136) (Qiagen Inc., CA, USA); and glucose assay kit, insulin ELISA kit, glycerol 3-phosphate activity kit, and lactate dehydrogenase (LDH) activity kit (BioVision Inc., CA, USA).

### 2.2. Cell lines

C2C12 mouse myoblast, 3T3L1 mouse preadipocyte, and BTC6 mouse beta cell lines were grown in DMEM medium containing 10%, 10%, and 15% inactivated FBS, respectively, and 1% penicillin/streptomycin at 37 °C in a humidified environment containing 5% $CO_2$. HepG2 human liver and Caco-2 human colon cell lines were grown in EMEM medium containing 10% and 5% inactivated FBS, respectively, and 1% penicillin/streptomycin at 37 °C in a humidified environment containing 5% $CO_2$. When the cells reached 80% confluency, they were removed with a trypsin-EDTA solution, stained with trypan blue, and counted on a Thomacell counting chamber using the microscope for subculturing.

### 2.3. Test compounds – alysine A and alysine B

#### 2.3.1. Isolation and purification

Test compounds alysine A and alysine B were isolated from the aerial parts of *Teucrium alyssifolium*, and identified as described previously [22]. The plant was macerated with acetone, and the crude acetone extract was separated over silica gel using hexane, ethyl acetate, and ethanol, respectively. The collected fractions were further separated on small columns using Si-gel and Sephadex LH-20, in addition to preparative TLC plates. The structure of the alysine A and alysine B were confirmed based on X-ray diffraction, 1D- and 2D-NMR, and mass spectral analyses [22] (Figures S1–S10, Table S1), (Figure 1).

### 2.4. Preparations for use in the test experiments

All of the test compounds were first solubilized in DMSO, with a final concentration of 1 mg/mL, and completed to the final volume with the growth medium. The DMSO concentration was adjusted to 10% in the final volume. The dissolved compounds were then aliquoted into small volumes, gassed with nitrogen, and stored at –20 °C. During the experiments, each aliquot was opened and used for testing the activities, and the remaining quantities were discarded. Thus, the compounds were impaired during the experiments or prevented from being exposed to oxidation. Hence, deterioration or oxidation of the compounds during the experiments was prevented.

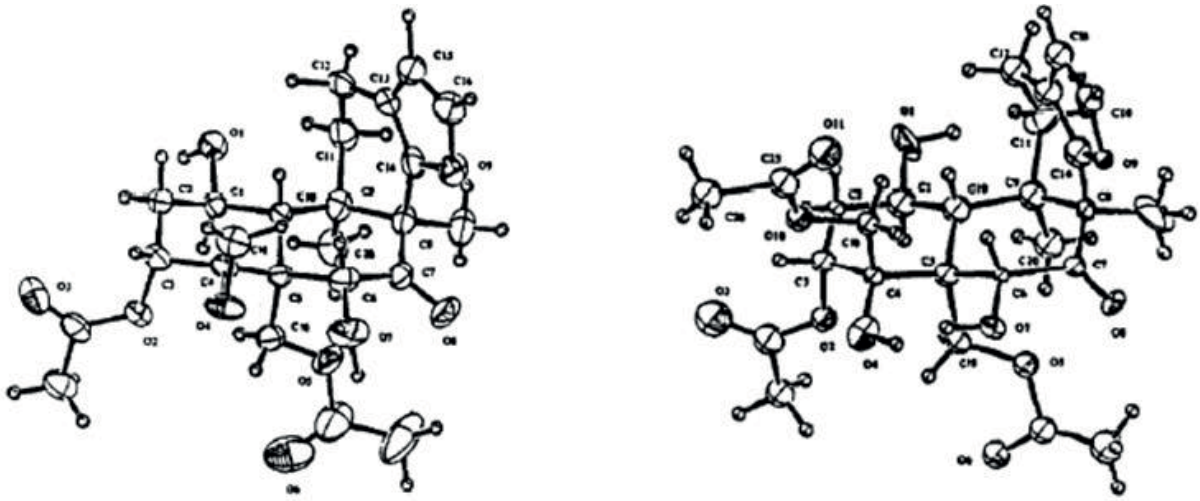

**Figure 1**. X-ray spectra of alysine A and alysine B.

### 2.5. Effect on cell viability

The cells were plated in 96-well plates at $1 \times 10^4$ cells/well and supplemented with the appropriate growth medium to give a total of 200 $\mu$L. The cells were allowed to adhere to the plate. Next, the growth medium was poured off and the test compounds were added into the wells, at various concentrations, along with the vehicle controls (10% DMSO in growth medium), and incubated for 24 h in a $CO_2$ incubator. At the end of this period, 100 $\mu$L of crystal violet solution (0.5% in 10% EtOH) was added to each well after aspirating the test compounds, and they were then incubated at room temperature for 10 min. The stain was then washed out under tap water until the stain was removed. Next, 100 $\mu$L of sodium citrate solution (dissolved in 50% EtOH, 1 M, pH 4.2) was added to the wells and incubated at room temperature for 15 min. The absorbance values were then measured at 630 nm using an ELISA microplate reader with agitation. The percent survival was determined using the obtained absorbance values.

### 2.6. LDH cytotoxicity assay

In addition to crystal violet staining, the LDH activities were measured in the medium where the cells were incubated with the test compounds, if there was any toxic effect on the cells at the concentrations determined. LDH activities in the medium were determined colorimetrically using the BioVision LDH-cytotoxicity colorimetric assay kit, as directed by the manufacturer.

### 2.7. Glucose uptake test

Glucose uptake experiments were performed with the 3T3-L1*, C2C12, and Chang cell lines. For these experiments, freshly passaged cells were seeded at 4500 cells per well in a 96-well microplate and grown for 48 h. At the end of this period, 8 mM glucose, 0.1% BSA, and the test compound or vehicle (10% DMSO in the medium) or positive controls (1 $\mu$M insulin and 1 $\mu$M metmorfin) were added to the appropriate well and incubated for an additional 2 h. At the end of the incubation period, 10 $\mu$L of the medium was transferred from each well into a new 96-well microplate. The final volume was brought to 200 $\mu$L by adding glucose reactant, and the absorbances were recorded at 450 nm using a microplate reader after 30 min incubation at 37 °C. The glucose assay was determined by essentially using the BioVision colorimetric glucose assay kit, following the

manufacturer's instructions.

The *3T3-L1 preadipocytes were transformed into adipocytes for use in the glucose uptake tests. Adipocyte differentiation was induced by adding 10 $\mu$g/mL insulin, $10^{-8}$ M DEX, and 0.1 mM isobutylmethylxanthine to the growth medium of the freshly passaged 3T3-L1 cells at the end of the first day. At the end of the fifth day, the cells were washed and transferred to normal growth medium. Cell differentiation was determined using the highly sensitive BioVision glycerol-3-phosphate dehydrogenase (G3PDH) activity colorimetric assay kit, as directed by the manufacturer, since G3PDH mRNA, protein, and activity are used as an indicator of adipocyte differentiation.

### 2.8. Glucose utilization (glycogen content) test

These experiments were performed with C2C12 muscle and HepG2 liver cell lines that had a glycogen storage capacity. The cells were grown under standard conditions until the day of the experiment. On the day of the experiment, the cells were washed with PBS at 37 °C, to remove the residues of the glucose and medium, and incubated for 2 h in serum-free medium. The cells were then incubated with the growth medium, vehicle, positive control agent (1 $\mu$M insulin), or test compounds. At the end of the incubation time, the cells were trypsinized and counted using a hemocytometer to remove $1.0 \times 10^6$ cells, which were then centrifuged (4 min at 5 °C, 800 × $g$). The resulting pellet was resuspended by homogenization in 200 $\mu$L of distilled water on ice and then boiled for 5 min to inactivate the glycogen degrading enzymes. The boiled suspension was then spun at 18,000 × $g$ for 10 min, and 25 $\mu$L of the supernatant was transferred to 96-well plates, and the glycogen content was determined in a colorimetric manner, in accordance with the manufacturer's instructions, with the BioVision glycogen assay kit.

### 2.9. Glucose transport test

These experiments were performed with the Caco-2 cell line. The glucose transport activity of the Caco-2 cell lines was performed with the previous method. For the transport experiments, the cells were plated in polycarbonate-filtered cell culture plates (Corning Transwell, 24-mm diameter, 3 $\mu$m), as described by [23], and the cells were left to differentiate for 15–17 days after confluency; the medium was regularly changed 3 times a week. The integrity of the Caco-2 cell monolayers and the full development of the tight junctions were monitored by microscopic examination. In order to measure the glucose transport across the Caco-2 monolayer, both sides of the transwells were washed with buffer (20 mM Tris-HCl, pH 7.4 containing 80 mM NaCl, 100 mM mannitol, 3 mM $K_2HPO_4$, 1 mM $CaCl_2$, and 1 mg/mL BSA) to remove any traces of glucose. The monolayer was then subjected to preincubation in the incubation buffer at 37 °C for 1 h and replaced with fresh incubation buffer just before the transport assay. The transport experiment was initiated by the addition of 25 mM D-glucose plus the vehicle control, positive control (1 $\mu$M insulin), or test compounds to the apical side of the chamber. Next, 10 $\mu$L of the samples were taken at 0, 30, and 60 min from the apical and basolateral sides, and replaced with glucose-free incubation solution. Glucose levels in the samples were determined using the BioVision colorimetric glucose assay kit, according to the manufacturer's instructions.

### 2.10. Glucose absorption ($\alpha$-glucosidase activity) test

The assay was performed with the Caco-2 cell line, as described by [24], under the described conditions given above in Section 4.7. To determine the alpha-glycosidase activity in the Caco-2 cells, the trans-wells were

washed with PBS. The monolayer was subjected to preincubation in PBS at 37 °C for 1 h. The experiment was initiated by changing the apical medium with 28 $\mu$M maltose, 28 $\mu$M sucrose, and PBS containing a vehicle, positive control (1 $\mu$M glibenclamide), or the test compounds. Only PBS was added to the basal side. After the cells were incubated for 2 h under these conditions, 50 $\mu$L of sample from the apical side was quantitated for the glucose concentration using the BioVision colorimetric glucose assay kit to determine the amount of glucose liberated by the alpha-glycosidase.

### 2.11. Insulin secretion test

In order to determine the effects of the test compound on insulin secretion under normal or hyperglycemic conditions, freshly passaged BTC6 cells were plated into 96-well microplates at $1 \times 10^4$ cells/well and incubated under appropriate conditions for 2 days. At the end of that period, each well was washed twice with 200 $\mu$L Krebs-ringer-bicarbonate-HEPES buffer (KRBH: 118, 4 mM NaCl, 4.75 mM KCl, 1.192 mM $MgSO_4$, 2.54 mM $CaCl_2$, 10 mM HEPES, 2 mM $NaHCO_3$, 0.1 % BSA). The cells were then incubated in 200 $\mu$L KRBH buffer for 30 min at room temperature. Next, the medium was removed and the wells were incubated at room temperature for 45 min in KRBH containing either a vehicle, positive control (1 $\mu$M glibenclamide), or test compounds in the presence or absence of 33.3 mM glucose. After the incubation period, 20 $\mu$L of sample from each well was transferred into a fresh 96-well plate and the amount of insulin in the medium was determined using the highly-sensitive Millipore rat/mouse insulin colorimetric ELISA kit, as directed by the manufacturer's instructions.

### 2.12. Quantitative analyses of the transcripts in insulin signaling and glucose metabolism

Determination of the expression level of the genes involved in glucose metabolism and insulin signaling was determined by treating the appropriate cell lines with the test compounds.

### 2.13. RNA isolation and cDNA synthesis

The total RNA was isolated from the cell lines using the RNeasy plus universal mini kit, following the manufacturer's instructions, and was checked on a 1.5% (w/v) agarose gel stained with ethidium bromide and visualized under ultraviolet light (DNR Bioimaging Systems Ltd., Neve Yamin, Israel). The RNA concentration and purity were determined by measuring the optical density at ratios of 260/280 and 260/230 using a Nano Spectrophotometer (Maestrogen Inc., Taiwan, R.O.C.). RNA was reverse transcribed using the EasyScript™plus cDNA Synthesis kit. The reaction mixture was incubated for 50 min at 50 °C, followed by termination by heating at 5 min at 85 °C. The cDNA concentration was measured with a Nanodrop and distributed in aliquots before storing at −80 °C.

### 2.14. qPCR quantification assays

The high-quality, ISO9001 certificated, custom-designed gene-specific primers had been synthesized by GenScript (Piscataway, NJ, USA). These validated primers were used for profiling the differential gene expression between separate treatment groups. Positive and negative controls, along with the housekeeping genes, were applied for qPCR reactions for the normalization of target gene expression. After assuring the integrity, purity and the quality of the cDNA, the whole volume of synthesized cDNA was used for the qPCR protocol. Enough master mix, using KiloGreen 2X qPCR master mix, was prepared and run under the optimized thermal cycling parameters on a Exicycler 96 Thermal Block (Bioneer, Corp., Daejeon, Korea).

### 2.15. Statistical analyses

Statistical analyses were carried out by applying Student's t-test using the GraphPad Prism 6.0 statistical software package for Windows (GraphPad Software, Inc., CA, USA). Statistical significance was accepted as $P < 0.05$ and the values were expressed as the mean ± standard deviation. The qRT-PCR data analysis web portal (Qiagen, version 3.5) was applied. Values of the cycle threshold (Ct) obtained in the quantification were used for calculations of the fold changes in mRNA abundance according to the $2^{-\Delta\Delta Ct}$ method [25].

## 3. Results and discussion

The data obtained from the present study were given as the mean ± standard deviation of the repeated experiments. Unless otherwise specified, all of the data were the average of at least 3 independent repeats of triplet measurements. Molecular structures and the properties of the test compounds are given in Figure 2.


**Figure 2**. Chemical structures of the test compounds, alysine A and alysine B.

### 3.1. The effect on cell viability

It was primarily aimed to determine the nontoxic doses. In preclinical toxicology studies, $EC_{10}$ (the dose lethal to 10% of the cell treated) represents a safe phase I trial starting dose and EC values for humans are best estimated for human cell cultures. Therefore, the $EC_{10}$ dose for alysine A and alysine B in the cell lines was investigated by crystal violet staining. Figure 3 shows the cell viability, ranging from 0 to 1 mM for alysine A and alysine B, respectively. As is obvious from Figure 3, the $EC_{10}$ values were almost equal, and the average of the calculated $EC_{10}$ values for the different cell lines was used throughout the study for all of the cell lines, i.e. 0.087 mM for alysine A and 0.075 mM for alysine B. Furthermore, the LDH leakage assay, based on the measurement of the LDH activity in the extracellular medium, was performed to evaluate the effect of the selected doses in all of the examined cell lines (Table 1).

**Table 1**. Effects of the test compounds on LDH activity in the extracellular medium of the cell lines.

| **Treatment** | **LDH activity in the extracellular medium (mU/mL)** | | | | |
|---|---|---|---|---|---|
| | BTC6 | C2C12 | 3T3-L1 | HepG2 | Caco-2 |
| **Control** | 61.2 ± 7.67 | 52.0 ± 4.3 | 50.6 ± 6.48 | 78.2 ± 3.21 | 41.6 ± 5.43 |
| **Alysine A** | 57.4 ± 3.62 | 54.4 ± 0.72 | 58.8 ± 3.73 | 81.5 ± 1.80 | 47.8 ± 2.67 |
| **Alysine B** | 66.9 ± 3.68 | 49.6 ± 2.71 | 56.1 ± 5.58 | 62.7 ± 1.78 | 38.2 ± 3.39 |

### 3.2. Effect on the glucose uptake

The 3 cell lines were incubated with the test compounds, along with the control and positive control agents, and then the remaining glucose concentration was determined in the extracellular medium. The cells were exposed

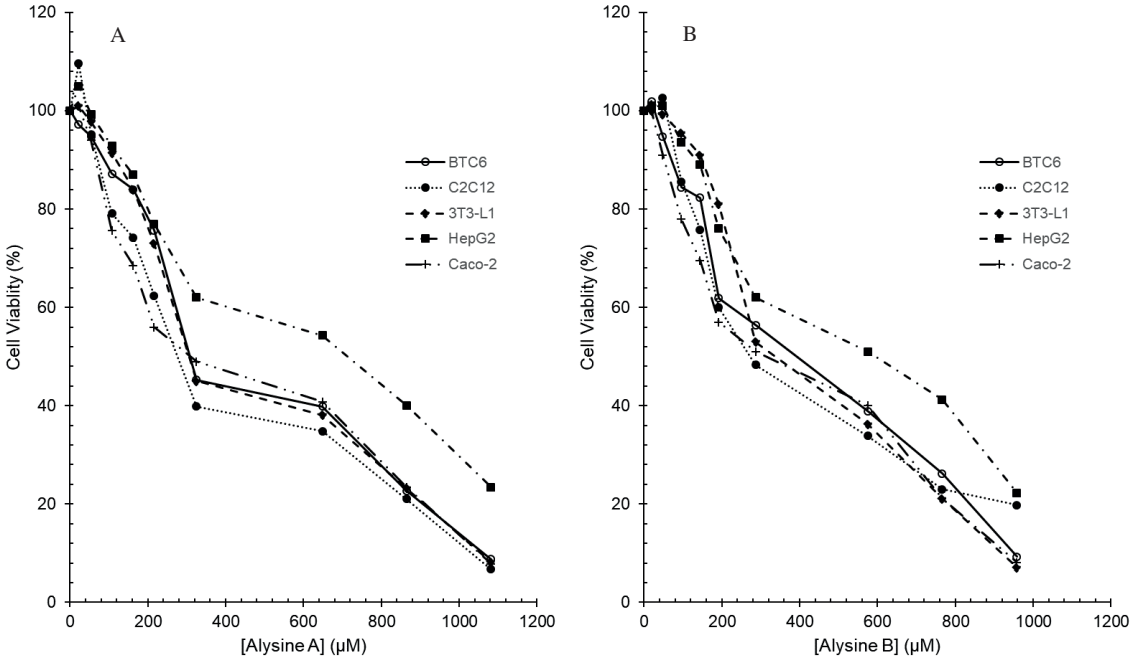


**Figure 3**. Cytotoxic response of the different cell lines to alysine A (part A) and alysine B (part B). The dose-response curve was used to estimate the $EC_{10}$ values.

to 1 $\mu$M insulin, 1 $\mu$M metformin, and the test compounds for 2 h. Both test compounds significantly increased the glucose uptake in the muscle and liver cell lines, whereas they showed little effect on the adipocytes (Table 2). The increment levels were higher with alysine A than with alysine B, and it was comparable and equal to the increments exerted by both the insulin and metformin.

**Table 2**. Remaining glucose concentrations in the extracellular medium of the C2C12 muscle, HepG2 liver, and 3T3-L1 adipocyte cells after 2-h incubation with the test compounds.

| **Treatment** | **Remaining glucose concentration in the extracellular medium ($\mu$g/mL)** | | |
|---|---|---|---|
| | C2C12 | HepG2 | 3T3-L1* |
| **Control** | 12.4 ± 2.1 | 10.8 ± 2.8 | 13.4 ± 1.1 |
| **Metformin** | 1.84 ± 0.06$^a$ | 2.05 ± 0.19$^a$ | 7.30 ± 0.98$^a$ |
| **Insulin** | 2.25 ± 0.10$^a$ | 2.27 ± 0.07$^a$ | 8.23 ± 0.62$^a$ |
| **Alysine A** | 2.02 ± 0.19$^a$ | 2.48 ± 0.13$^a$ | 10.38 ± 1.22$^b$ |
| **Alysine B** | 3.36 ± 0.40$^a$ | 3.39 ± 0.48$^a$ | 11.94 ± 1.40$^c$ |

*Adipocyte differentiation of the preadipocyte cells were confirmed by observing 8.4-fold induction of the G3PDH activity (preadipocytes: 4.94 ± 0.72 and differentiated adipocytes: 41.6 ± 2.68). $^a$: $P < 0.0001$, $^b$: $P < 0.001$, $^c$: $P < 0.05$.

### 3.3. The effects on glucose utilization (glycogen content)

The effect of the test compounds, as well as the insulin on glucose utilization, in the C2C12 and HepG2 cells, was assessed by measuring the amount of glucose stored as glycogen. The amount of intracellular glycogen content was significantly increased by both alysine A and alysine B in both cell lines (Table 3). As seen in the glucose uptake, the increments were higher with alysine A than alysine B, and it was even higher than the insulin effect.

**Table 3**. Quantities of glycogen stored by the positive control and test compounds in the C2C12 muscle and HepG2 liver cell lines.

| **Treatment** | **Intracellular glycogen concentration per 1.0 × $10^6$ cells ($\mu$g/mL)** | |
|---|---|---|
| | C2C12 | HepG2 |
| **Control** | 0.232 ± 0.011 | 0.185 ± 0.015[a] |
| **Insulin** | 0.534 ± 0.031[a] | 0.305 ± 0.018[a] |
| **Alysine A** | 0.717 ± 0.080[a] | 0.591 ± 0.087[a] |
| **Alysine B** | 0.507 ± 0.071[a] | 0.432 ± 0.051[a] |

[a]: P < 0.0001.

### 3.4. The effect on glucose transport

Via utilization of the confluent and differentiated Caco-2 cell monolayer, the impact of the test compounds on the glucose uptake in the human Caco-2 cells was examined. The Caco-2 cell monolayers with intact, tight, junctions displayed a consistent rate of glucose transport, as given in Table 4. Both alysine A and alysine B exerted a significant stimulatory impact on the glucose transport over the Caco-2 monolayers. However, on the contrary to the other effects seen with test compounds, the stimulation on the glucose uptake was almost as twice as high with alysine B than with alysine A.

**Table 4**. Temporal glucose concentrations on the apical and basolateral surfaces of the Caco-2 cell monolayer treated either with the positive control or test.

| **Treatment** | **Glucose concentration ($\mu$g/mL) apical side** | | | **Glucose concentration ($\mu$g/mL) basolateral side** | | |
|---|---|---|---|---|---|---|
| | 0 min | 30 min | 60 min | 0 min | 30 min | 60 min |
| **Control** | 1.68 ± 0.08 | 1.70 ± 0.11 | 1.61 ± 0.04 | 0.13 ± 0.05 | 0.27 ± 0.17 | 0.50 ± 0.32 |
| **Insulin** | 1.63 ± 0.10 | 1.61 ± 0.03 | 1.61 ± 0.06 | 0.09 ± 0.00 | 4.55 ± 0.37[a] | 6.79 ± 0.42[a] |
| **Alysine A** | 1.70 ± 0.16 | 1.88 ± 0.02 | 1.65 ± 0.06 | 0.30 ± 0.00 | 3.80 ± 0.32[a] | 7.29 ± 0.51[a] |
| **Alysine B** | 1.73 ± 0.03 | 1.58 ± 0.09 | 1.69 ± 0.10 | 0.11 ± 0.01 | 3.53 ± 0.24[a] | 14.06 ± 0.91[a] |

[a]: P < 0.0001.

### 3.5. The effect on glucose absorption ($\alpha$-glucosidase activity)

The effect of the test compounds on the release of glucose by $\alpha$-glucosidase was determined in the Caco-2 cell monolayer. Neither of the test compounds showed inhibition of the sucrose hydrolysis activity of $\alpha$-glucosidase with the Caco-2 monolayer (Table 5).

**Table 5**. Glucose concentrations released by $\alpha$-glycosidase at the apical surface of the Caco-2 cells in the presence of the different test compounds.

| **Treatment** | **Glucose concentration ($\mu$g/mL)** |
|---|---|
| Control | 0.080 ± 0.03 |
| Alysine A | 0.081 ± 0.08 |
| Alysine B | 0.084 ± 0.07 |

Glibenclamide was used as the positive control.

### 3.6. The effect on the insulin secretion

To study the effects of the test compounds on insulin secretion under normal or hyperglycemic conditions, confluent BTC6 cells, in 96-well microplates, were used. Prior to the insulin secretion assay, the cells were washed with KRBH and the culture media was changed, and the cells were then incubated with 8 mM glucose KRBH media (normal conditions) or 33 mM glucose KRBH media (hyperglycemic conditions), and exposed to experimental concentrations (Table 6) of the test compounds, as determined in the cell viability studies. After exposure, the insulin content was subsequently determined. Neither of the test compounds affected the insulin secretion under either of the normoglycemic or hyperglycemic conditions.

**Table 6**. Effect of alysine A and alysine B on the insulin secretion in the BTC6 cell.

| **Treatment** | **Insulin Concentration (ng/mL)** | |
|---|---|---|
| | 8 mM glucose | 33 mM glucose |
| Control | ND | ND |
| Glibenclamide | 4.1 ± 0.33 | 6.8 ± 0.71 |
| Alysine A | ND | ND |
| Alysine B | ND | ND |

ND: Not detectable.

### 3.7. The effect on the expression of the selected genes in glucose metabolism and insulin signaling

qPCR was applied to analyze the impact of the test compounds on the mRNA levels of the selected genes, which are known to be important in the regulation of glucose metabolism and insulin signaling. A detailed description of the genes and the primers used is given in Table S1. The expression levels of the genes were examined primarily in the muscle, liver, and adipocyte cell lines, which are of the most important in glucose homeostasis. In addition, several genes transcripts were also analyzed in the Caco-2 cell line, which were in relation to the genes associated with glucose transport. Similarly, only the expression levels of the GLUT2 and

insulin receptor substrate (IRS)-1 genes in the BTC6 cells were studied. Therefore, the genes expressed in the relevant cells were examined in the appropriate cell line (Table 7).

**Table 7**. Effects of alysine A (AA) and alysine B (AB) on the expression levels of various genes involved in the insulin pathway and glucose homeostasis in various cell lines.

| | **3T3-L1** | | **C2C12** | | **HepG2** | | **Caco-2** | | **BTC6** | |
|---|---|---|---|---|---|---|---|---|---|---|
| | AA | AB | AA | AB | AA | AB | AA | AB | AA | AB |
| **INSR** | 2.86 | 1.41 | –1.25 | –2.80 | 1.18 | –1.01 | | | | |
| **IRS 1** | –1.27 | –1.56 | 1.16 | –2.08 | –1.86 | –2.43 | | | 10.20 | 1.14 |
| **IRS 2** | 2.79 | 2.90 | 3.62 | –1.10 | –4.61 | –5.12 | | | | |
| **PK** | 3.68 | 2.98 | 3.28 | –2.28 | 5.04 | 2.87 | | | | |
| **PEPCK** | 14.12 | 2.33 | 64.45 | 1.69 | 4.17 | 2.38 | | | | |
| **GLUT4** | 4.50 | 2.40 | 2.97 | –5.08 | | | | | | |
| **AKR** | 1.51 | 3.07 | 5.17 | 2.71 | 7.88 | 4.37 | | | | |
| **PI3K** | 5.84 | –1.41 | | | | | | | | |
| **G6P** | 2.97 | 1.55 | 3.75 | 1.02 | 1.05 | 1.05 | | | | |
| **AG** | | | | | | | –3.82 | –5.70 | | |
| **GLUT2** | | | | | | | –1.52 | –5.78 | 9.92 | 1.12 |
| **GLUT3** | | | | | | | 1.47 | | | |
| **GLUT5** | | | | | | | –2.29 | –2.93 | | |
| **SLGT1** | | | | | | | –4.52 | –2.20 | | |

Cells shaded with light gray filling show significantly ($P < 0.01$) different values.
Expression levels were given as fold changes, normalized relative to the control.
Positive values indicate increases, and negative values indicate decreases.

For the in vivo antidiabetic studies, hyperglycemic animal models were utilized. In vivo studies are vital and imperative to demonstrate the efficiency of new hypoglycemic agents and uncover the particular mechanism of action of compounds. However, since there are numerous systems by which the blood glucose level is regulated, and they are hard to control in animal models, various in vitro models arose as a more practical way to deal with the screening of potential antidiabetic agents. These models were essential in overcoming potential ethical issues, by reducing the unnecessary utilization of test animals, as well as surpassing financial constraints on animal supply and care. Testing compounds that confirmed efficacy in the in vitro models, and later in the animal models, were accepted as a more accurate strategy. Herein, a set of in vitro models was designed to explore the actions and mechanisms of potential antidiabetic compounds [26–28].

The present research explored the in vitro antidiabetic properties of 2 novel compounds isolated and characterized from endemic species *Teucrium alyssifolium*, with the aim of optimizing the techniques that were required for their testing and determining their efficacy. The study was based on the fact that extracts from *Teucrium* species are widely used as alternative and complementary medicine for T2DM. However, there is a lack of scientific evidence for their efficacy [11,12,29]. To provide a detailed examination of glucose homeostasis, appropriate cell lines, representing the specific metabolic pathways involved in glucose homeostasis, were used. These cell lines were the C2C12 muscle, HepG2 liver, 3T3-L1 preadipocyte, Caco-2 epithelium, and pancreatic $\beta$TC6 cells. Insulin, metformin (glucose utilization), and glibenclamide (insulin secretion) were used as the

positive controls to compare the effects of the test compounds.

In studies to identify and detect new antidiabetic agents, compounds should be dosed such that they do not exhibit toxic effects, as opposed to anticancer studies [30]. The doses to be used should be at levels that will not cause contraindications to the in vivo systems and show no toxic effects, both in the model systems and in advanced studies. For this reason, we identified $EC_{10}$ as a safe phase I trial starting dose, and EC values for humans are best estimated for human cell cultures. Moreover, the no observed effect level and lowest observed effect level values were not detected with the cell lines [31]. These nontoxic values were used throughout the studies. The LDH test also confirmed that the determined dose values of the test compounds used in the model mechanisms did not exhibit toxic effects (Table 1). The LDH test confirmed that the selected doses did not disrupt the integrity of the cells, and thus were nontoxic. These results also demonstrated that there was no deterioration in the structural integrity of the cells.

When we examine the effects of alysine A and alysine B on the glucose uptake in the C2C12, HepG2, and 3T3-L1 cells, we observed that both compounds increased the glucose uptake higher than the metformin and insulin in all 3 cell lines (Table 2). Normally, at the physiological level, the muscle cell is the most highly expressed by the GLUT4 transporter (gene expression/activity chart; BioGPS.org). In our experiments, the observation of the highest glucose uptake in the adipocyte cells may have been due to an excessive increase in GLUT4 expression level, while the preadipocyte cells were differentiated to adipocyte cells. Since glucose uptake is an essential process for studying cell signaling and glucose metabolism [32,33], the strong positive influences observed with alysine A and alysine B are important for their antidiabetic efficacy and are promising for their expected activity in the in vivo system. It is possible to say that alysine A and alysine B are most likely to act on GLUT4, since the common point among the 3 cell types is the accelerated glucose transport into the cell by increasing the GLUT4 activity (GLUT4 translocates to the cell surface).

Our test compounds, on which the effects on glucose uptake were tested, also investigated the effects of glucose on the glucose storage model, which is another important parameter of glucose homeostasis. For this purpose, amounts of glycogen were determined in the model cell lines with glycogen storage capacity, the C2C12 muscle and HepG2 liver cell lines, when compared to the positive controls. In these experiments, results were obtained in parallel with previous glucose uptake. It was observed that the alicyclic compounds alysine A and alysine B significantly increased the amounts of stored glycogen in both cell lines, and significantly more than the positive control insulin ratio. The results from this and previous glucose uptake assays strongly supported that both compounds induced GLUT4 translocation through the protein kinase B (AKT) pathway by acting on IR, and also activate the pathway of glycogenesis via AKT. Of course, further experimentation is needed to support this model. It was also difficult to make a suggestion that such an effect was seen only in the liver cells and to suggest a possible model mechanism.

New agents have been tested for their effect on the insulin section, since the glucose homeostasis was maintained by a balance between insulin secretion and insulin action. For this reason, both alysine A and alysine B were tested for their impact on insulin secretion under normal or hyperglycemic conditions using the BTC6 cells. Neither of the test compounds affected the insulin secretion under either of the normoglycemic or hyperglycemic conditions.

The key enzymes and proteins within the regulation of glucose homeostasis were investigated to explore the antihyperglycemic impact and the mechanism of the test compounds. Both compounds increased the expression of the genes that were activated by the insulin in the tested cell lines. As mentioned previously above, 3 cell lines were investigated to obtain a detailed examination of glucose homeostasis. The insulin

receptor (INSR), IRS2, protein kinase (PK), GLUT4, and phosphoinositide 3-kinase (PI3K) expression levels were significantly increased in the 3T3-L1, C2C12, and HepG2 cells. These are significant genes involved in the insulin signaling pathway, favoring the antidiabetic action [34,35]. IRS is the adaptor protein recruited by the INSR and exhibits binding sites for diverse signaling companions. One of the signaling companions is the PI3K, which has a major role in insulin functions. It mediates one of the most important metabolic actions of insulin by translocating the GLUT4 from intracellular storage vesicles to the plasma membrane, thereby increasing glucose uptake into the skeletal muscle and adipose tissue [32,36]. Therefore, the results of the gene expression studies further confirmed our previous suggestion that these compounds induced GLUT4 translocation through the PI3K/AKT pathway by acting on IR, and also activated the pathway of glycogenesis via AKT. However, the opposite expression pattern was displayed with phosphoenolpyruvate carboxykinase (PEPCK), which is the key and regulatory enzyme in gluconeogenesis. The regulation of PEPCK is highly complex, as its promoter region contains many binding sites for transcriptional regulators modulated by glucagon, catecholamines, glucocorticoids, and insulin. It is also known that the repression of PEPCK gene expression by glucose is insulin-independent, but requires glucose metabolism [37]. Therefore, further studies using higher concentrations of glucose or pretreatment of the cells with glucose are required to resolve this discrepancy. Nevertheless, the majority of the tested genes illustrated an expression pattern supporting the antihyperglycemic impact of alysine A and alysine B. Aside from the expression of the transporter genes in the Caco-2 cell line, the expression level of the genes in the muscle, liver, adipocyte, and pancreatic cells was in favor of antidiabetic impact, contrary to a few genes like PEPCK.

As a conclusion, alysine A, and to lesser extent, alysine B, exercised significant and positive results on glucose homeostasis, and is a natural and pleiotropic antidiabetic agent. The cyclic and aliphatic side chains on the first ring of both compounds may have been responsible for the differences seen in the bioactivity of the 2 compounds. Advanced in vivo studies are required to completely clarify the impact of this compound on glucose homeostasis.

**Acknowledgments**

This work was supported by the Scientific and Technological Research Council of Turkey under TÜBİTAK, under Project No.: 114Z640, and Pamukkale University under Project No.: PAUBAP-2014FBE029.

## References

1. Twaij HA, Albadr AA, Abul-Khail A. Anti-ulcer activity of *Teucrium polium.* International Journal of Crude Drug Research 1987; 25: 125-128. doi: 10.3109/13880208709088138
2. Çakır A, Mavi A, Kazaz C, Yıldırım A, Küfrevioğlu ÖI. Antioxidant activities of the extracts and components of *Teucrium orientale* L. var. *orientale.* Turkish Journal of Chemistry 2006; 30 (4): 483-494.
3. Topcu G, Eris C. Neo-Clerodane diterpenoids from *Teucrium alyssifolium.* Journal of Natural Products 1997; 60: 1045-1047. doi: 10.1021/np9607060
4. Danaei G, Finucane MM, Lu Y, Singh GM, Cowan MJ et al. National, regional, and global trends in fasting plasma glucose and diabetes prevalence since 1980: systematic analysis of health examination surveys and epidemiological studies with 370 country-years and 2.7 million participants. Lancet 2011; 378: 31-40. doi: 10.1016/S0140-6736(11)60679-X
5. Mathers CD, Loncar D. Projections of global mortality and burden of disease from 2002 to 2030. PLOS Medicine 2006; 3: 2011-2030. doi: 10.1371/journal.pmed.0030442

6. Liu C, Wong P, Lii C, Hse H, Sheen L. Antidiabetic effect of garlic oil but not diallyl disulfide in rats with streptozotocin-induced diabetes. Food and Chemical Toxicology 2006; 44: 1377-1384. doi: 10.1016/j.fct.2005.07.013
7. Nandi A, Kitamura Y, Kahn CR, Accili D. Mouse models of insulin resistance. Physiological Reviews 2004; 84: 623-647. doi: 10.1152/physrev.00032.2003
8. Saltiel AR, Kahn CR. Insulin signaling and the regulation of glucose and lipid metabolism. Nature 2001; 414: 799-806. doi: 10.1038/414799a
9. Zelezniak A, Pers TH, Soares S, Patti ME, Patil KR. Metabolic network topology reveals transcriptional regulatory signatures of type 2 diabetes. PLOS Computational Biology 2010; 6: 1-13. doi: 10.1371/journal.pcbi.1000729.
10. Bailey CJ, Day C. Traditional plant medicines as treatments for diabetes. Diabetes Care 1989; 12: 553-564. doi: 10.2337/diacare.12.8.553
11. Gharaibeh MN, Elayan HH, Salhab AS. Hypoglycemic effects of *Teucrium-polium*. Journal of Ethnopharmacology 1988; 24: 93-99. doi: 10.1016/0378-8741(88)90139-0
12. Lv HW, Zhu MD, Luo JG, Kong LY. Antihyperglycemic glucosylated coumaroyltyramine derivatives from *Teucrium viscidum*. Journal of Natural Products 2014; 77: 200-205. doi: 10.1021/np400487a
13. Ayar B, Sen A, Topcu G, Yilmaz A. Evaluation of anti-diabetic potential of circiliol and circilineol using CACO2 cell line. FEBS Journal 2016; 283: 377.
14. Genet C, Strehle A, Schmidt C, Boudjelal G, Lobstein A et al. Structure-activity relationship study of betulinic acid, a novel and selective TGR5 agonist, and its synthetic derivatives: potential impact in diabetes. Journal of Medicinal Chemistry 2010; 53: 178-190. doi:10.1021/jm900872z
15. Nugroho AE, Lindawati NY, Herlyanti K, Widyastuti L, Pramono S. Anti-diabetic effect of a combination of andrographolide-enriched extract of Andrographis paniculata (Burm f.) Nees and asiaticoside-enriched extract of *Centella asiatica* L. in high fructose-fat fed rats. Indian Journal of Experimental Biology 2013; 51: 1101-1108.
16. Pergola PE, Krauth M, Huff JW, Ferguson DA, Ruiz S et al. Effect of bardoxolone methyl on kidney function in patients with T2D and stage 3b-4 CKD. American Journal of Nephrology 2011; 33: 469-476. doi: 10.1159/000327599
17. Pergola PE, Raskin P, Toto RD, Meyer CJ, Huff JW et al. Bardoxolone methyl and kidney function in CKD with type 2 diabetes. New England Journal of Medicine 2011; 365: 327-336. doi:10.1056/NEJMoa1105351
18. Sen A, Ayar B, Topcu G, Yilmaz A. A promising novel antidiabetic compound: alysine-A. FEBS Journal 2016; 283: 97.
19. Yilmaz A, Crowley RS, Sherwood AM, Prisinzano TE. Semisynthesis and kappa-opioid receptor activity of derivatives of columbin, a furanolactone diterpene. Journal of Natural Products 2017; 80: 2094-2100. doi:10.1021/acs.jnatprod.7b00327
20. Yilmaz A, Boğa M, Topçu G. Novel terpenoids with potential anti-Alzheimer activity from *Nepeta obtusicrena*. Records of Natural Products 2016; 10: 530-541.
21. Yilmaz A, Çağlar P, Dirmenci T, Gören N, Topçu G. A novel isopimarane diterpenoid with acetylcholinesterase inhibitory activity from *Nepeta sorgerae*, an endemic species to the Nemrut Mountain. Natural Product Communications 2012; 7: 693-696.
22. Topcu G, Eris C, Ulubelen A, Krawiec M, Watson WH. New rearranged neoclerodane diterpenoids from *Teucrium-alyssifolium*. Tetrahedron 1995; 51: 11793-11800. doi: 10.1016/0040-4020(95)00740-Y
23. Artursson P. Epithelial transport of drugs in cell-culture .1. A model for studying the passive diffusion of drugs over intestinal absorptive (caco-2) cells. Journal of Pharmaceutical Sciences 1990; 79: 476-482. doi: 10.1002/jps.2600790604
24. Huang YN, Zhao DD, Gao B, Zhong K, Zhu RX et al. Anti-hyperglycemic effect of chebulagic acid from the fruits of *Terminalia chebula* Retz. International Journal of Molecular Sciences 2012; 13: 6320-6333. doi:10.3390/ijms13056320

25. Livak KJ, Schmittgen TD. Analysis of relative gene expression data using real-time quantitative PCR and the 2(T)(-Delta Delta C) method. Methods 2001; 25: 402-408. doi: 10.1006/meth.2001.1262

26. Dsouza D, Lakshmidevi N. Models to study in vitro antidiabetic activity of plants: a review. International Journal of Pharma and Bio Sciences 2015; 6: 732-741.

27. Patel MB, Mishra SH. Cell lines in diabetes. Pharmacognosy Reviews 2008; 2: 188-205.

28. Skelin M, Rupnik M, Cencič A. Pancreatic beta cell lines and their applications in diabetes mellitus research. Altex 2010; 27: 105-113.

29. Esmaeili MA, Yazdanparast R. Hypoglycaemic effect of *Teucrium polium*: studies with rat pancreatic islets. Journal of Ethnopharmacology 2004; 95: 27-30. doi: 10.1016/j.jep.2004.06.023

30. Stein SA, Lamos EM, Davis SN. A review of the efficacy and safety of oral antidiabetic drugs. Expert Opinion on Drug Safety 2013; 12: 153-175. doi: 10.1517/14740338.2013.752813

31. Andersen ME. Toxicokinetic modeling and its applications in chemical risk assessment. Toxicology Letters 2003; 138 (1-2): 9-27. doi: 10.1016/S0378-4274(02)00375-2

32. Rowland AF, Fazakerley DJ, James DE. Mapping insulin/GLUT4 circuitry. Traffic 2011; 12: 672-681. doi: 10.1111/j.1600-0854.2011.01178.x

33. Yasuma T, Yutaka Y, D'Alessandro-Gabazza CN, Toda M, Gil-Bernabe P et al. Amelioration of diabetes by protein S. Diabetes 2016; 65: 1940-1951. doi: 10.2337/db15-1404

34. Cheng Z, Tseng Y, White MF. Insulin signaling meets mitochondria in metabolism. Trends in Endocrinology and Metabolism 2010; 21: 589-598. doi: 10.1016/j.tem.2010.06.005

35. Siddle K. Signaling by insulin and IGF receptors: supporting acts and new players. Journal of Molecular Endocrinology 2011; 47: R1-10. doi: 10.1530/JME-11-0022

36. Ramachandran V, Saravanan R. Glucose uptake through translocation and activation of GLUT4 in PI3K/Akt signaling pathway by asiatic acid in diabetic rats. Human & Experimental Toxicology 2015; 34: 884-893. doi: 10.1177/0960327114561663

37. Scott DK, O'Doherty RM, Stafford JM, Newgard CB, Granner DK. The repression of hormone-activated PEPCK gene expression by glucose is insulin-independent but requires glucose metabolism. Journal of Biological Chemistry 1998; 273: 24145-24151. doi: 10.1074/jbc.273.37.24145

**Supporting material**

All of the spectral data, including the 1D- and 2D-protons, and carbon NMR and X-ray spectra given below, were reported by [22].

Extraction and isolation of the compounds: dried and powdered aerial parts of the plant (1.4 kg) were extracted with acetone at room temperature, evaporated under a vacuum, and 72 g of a crude extract was obtained. The crude extract was chromatographed over silica gel using hexane, a gradient of ethyl acetate up to 100%, followed by ethanol. The collected fractions were combined after TLC control and further separated on small Si-gel and Sephadex LH-20 columns, as well as on preparative TLC plates. From the preparative TLC separation, alysine A (105 mg) and alysine B (200 mg) were obtained.

Alysine A: obtained as colorless crystals; it had a molecular formula of $C_{24}H_{30}O_9$, as determined by HR EIMS (m/z 462.1884). The structure was established based particularly on $^{1}H$ and $^{13}C$ NMR spectroscopic techniques, including spin decoupling, heteronuclear correlation (HETCOR), heteronuclear multiple bond correlation (HMBC), and Selective Insensitive Nuclei Enhanced by Polarization Transfer (SINEPT) experiments, and confirmed by X-ray analysis.

Alysine B: isolated as a colorless crystalline compound. The FAB and HR EIMS indicated a molecular formula of $C_{26}H_{34}O_{11}$ (m/z 522.2101). The structure was established based particularly on $^{1}H$ and $^{13}C$ NMR spectroscopic techniques, including 2D-NMR techniques.

**Table S1.** $^{1}H$ and $^{13}C$ NMR data of compounds alysine A and alysine B in $CDCl_3$.

| NMR Data | Alysine A | | Alysine B | |
|---|---|---|---|---|
| Position | $^{1}H$ | $^{13}C$ | $^{1}H$ | $^{13}C$ |
| 1 | 4.45 | 65.00 | 4.39 | 64.96 |
| 2 | 2.28; 1.92 | 40.60 | 2.42; 1.92 | 37.86 |
| 3 | 4.59 | 74.60 | 5.29 | 71.28 |
| 4 | - | 63.27 | - | 71.37 |
| 5 | - | 45.60 | - | 44.79 |
| 6 | 3.80 | 75.40 | 3.92 | 75.93 |
| 7 | - | 206.70 | - | 206.83 |
| 8 | - | 53.91 | - | 53.49 |
| 9 | - | 49.20 | - | 52.44 |
| 10 | 2.31 | 45.73 | 2.40 | 42.02 |
| 11 | 2.55 | 19.30 | 2.01; 2.42 | 18.94 |
| 12 | 1.61; 2.84 | 33.62 | 1.61; 2.84 | 34.45 |
| 13 | - | 116.30 | - | 116.54 |
| 14 | - | 151.90 | - | 151.21 |
| 15 | 6.24 | 110.44 | 6.22 | 110.25 |
| 16 | 7.37 | 142.50 | 7.38 | 142.45 |
| 17 | 1.34 | 19.19 | 1.42 | 18.08 |
| 18 | 3.08; 2.62 | 49.20 | 4.22; 4.06 | 66.21 |
| 19 | 4.27; 4.68 | 62.90 | 4.41; 5.15 | 65.50 |
| 20 | 1.14 | 17.82 | 1.21 | 17.49 |
| CO | - | 170.13 | - | 169.97 |
| $CH_3$ | 2.02 | 20.70 | 1.99 | 20.17 |
| CO | - | 169.70 | - | 169.59 |
| $CH_3$ | 2.06 | 20.91 | 2.05 | 20.49 |
| CO | - | - | - | 169.59 |
| $CH_3$ | - | - | 2.08 | 20.76 |

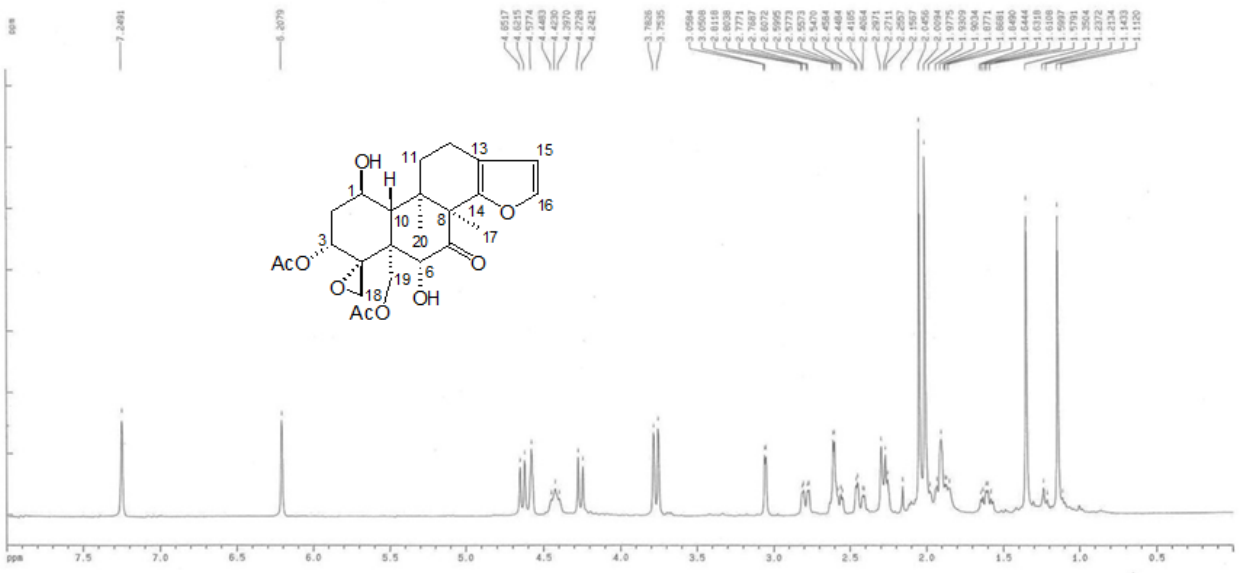


**Figure S1.** $^{1}H$ NMR Spectrum of alysine A ($CDCl_3$).

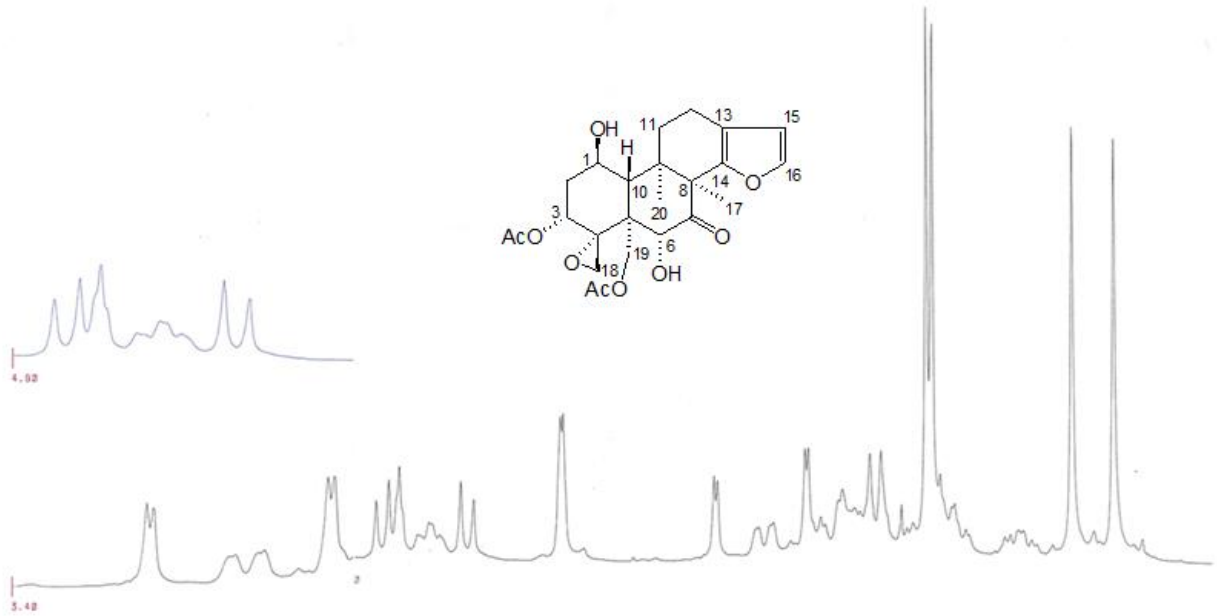


**Figure S2.** Enhanced $^{1}H$ NMR spectrum of alysine A ($CDCl_3$).

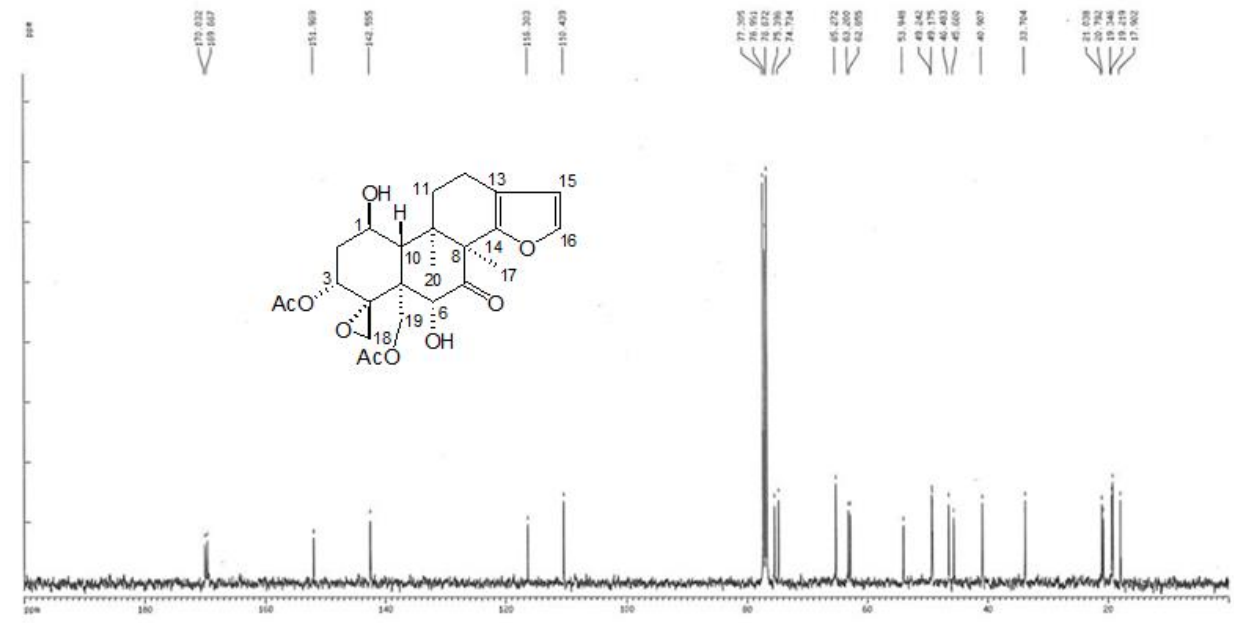


**Figure S3.** $^{13}C$ NMR (BB) spectrum of alysine A ($CDCl_3$).

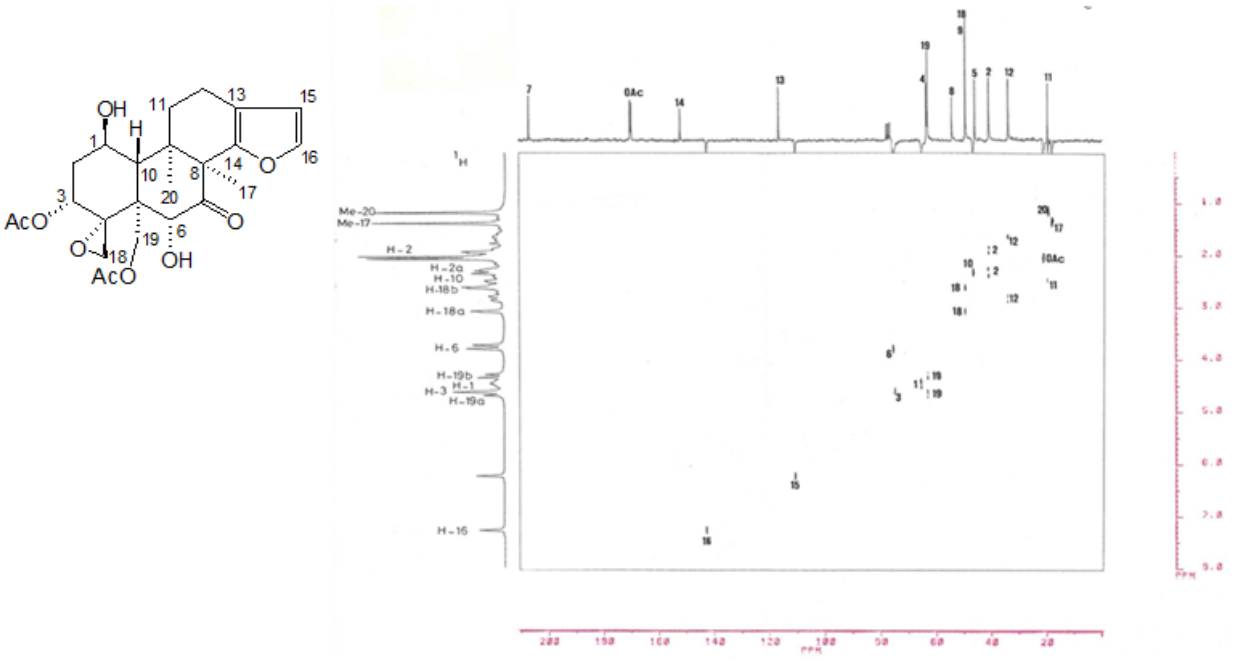


**Figure S4.** $^{1}H–^{13}C$ correlation (HETCOR) spectrum of alysine A.

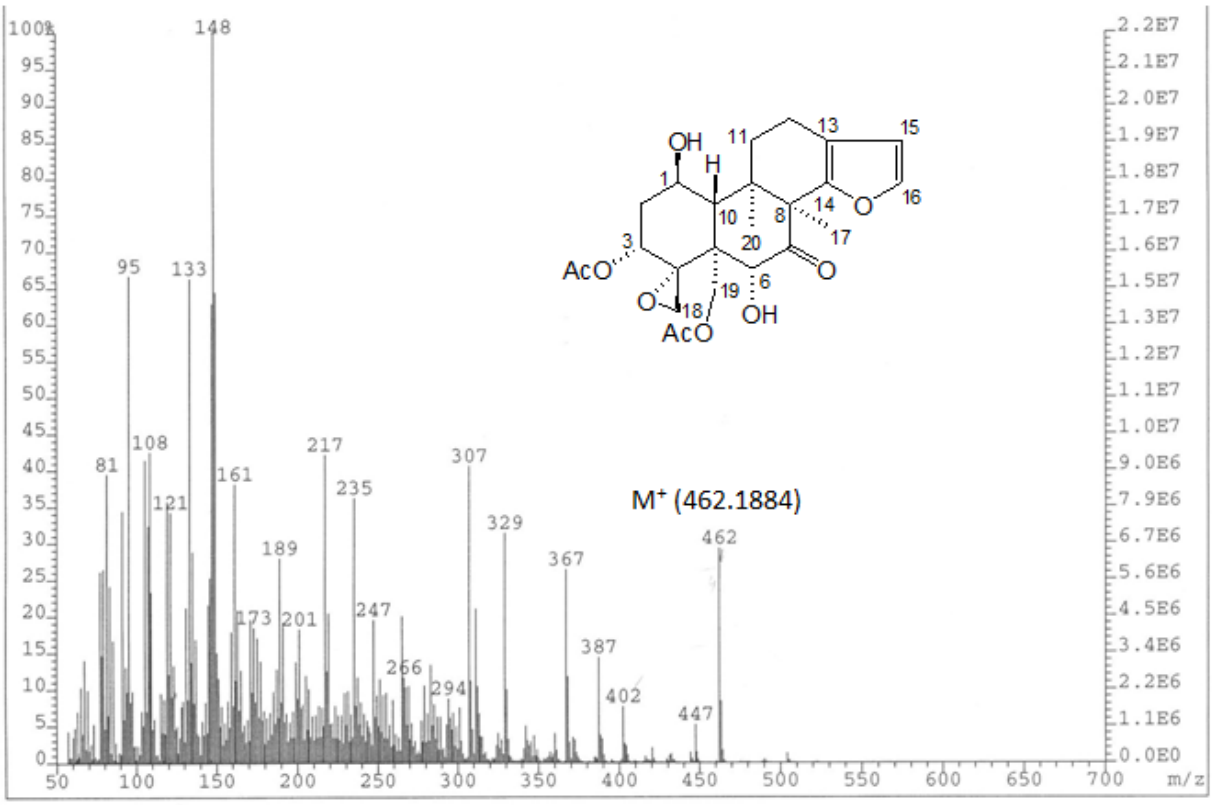


**Figure S5.** Mass (EI) spectrum of alysine A.

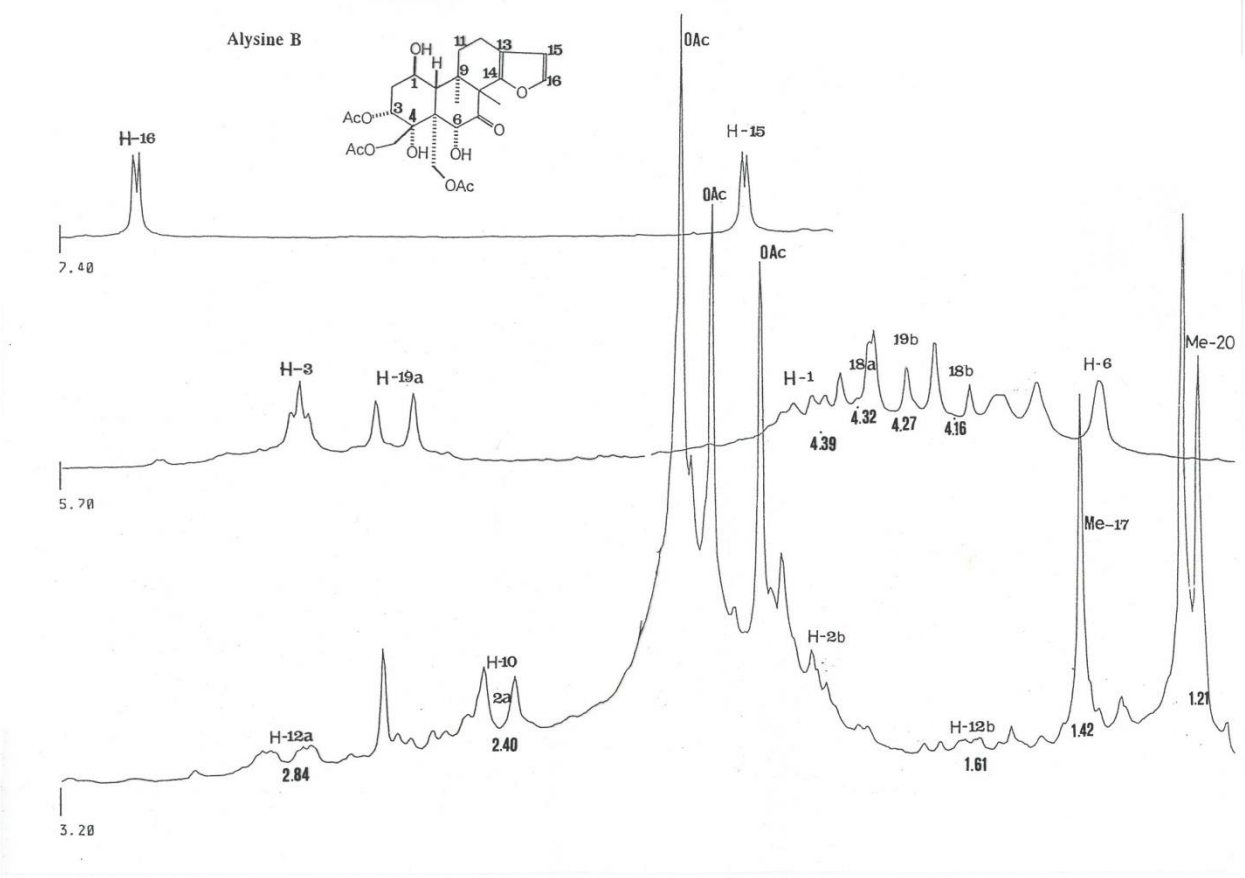


**Figure S6.** $^{1}$H NMR spectrum of alysine B ($CDCl_3$).

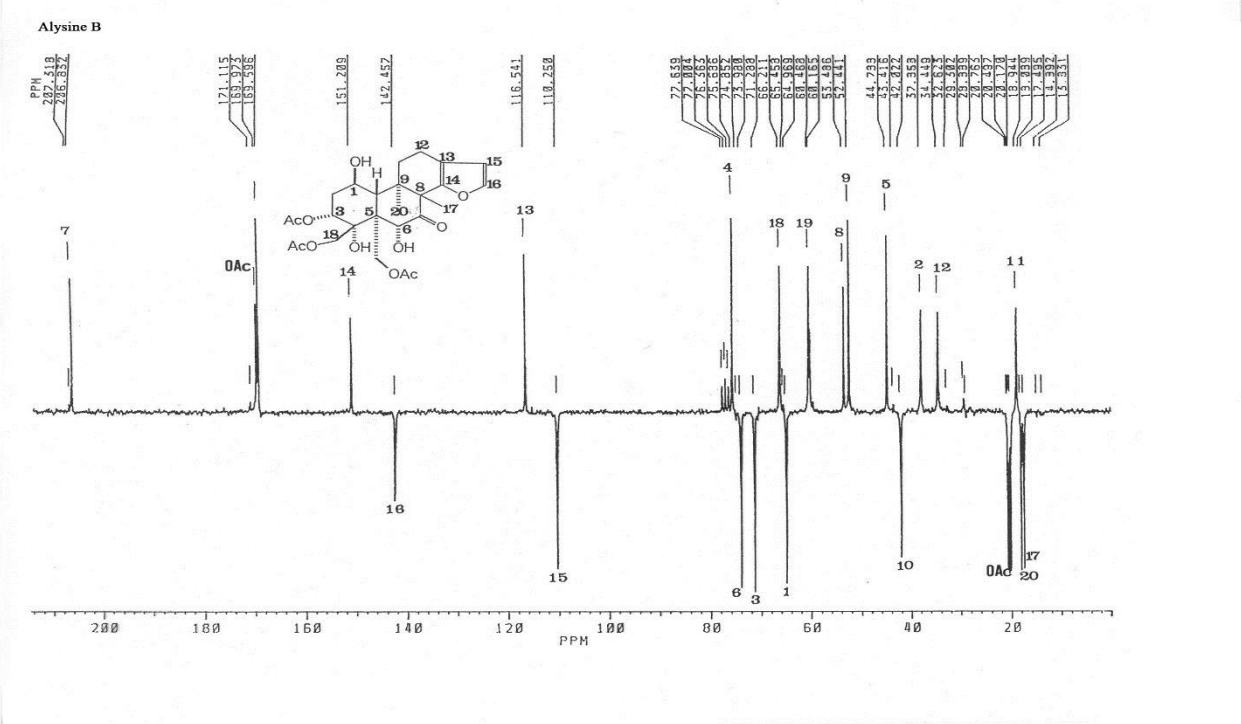


**Figure S7.** $^{13}C$ NMR (APT) spectrum of alysine B ($CDCl_3$).

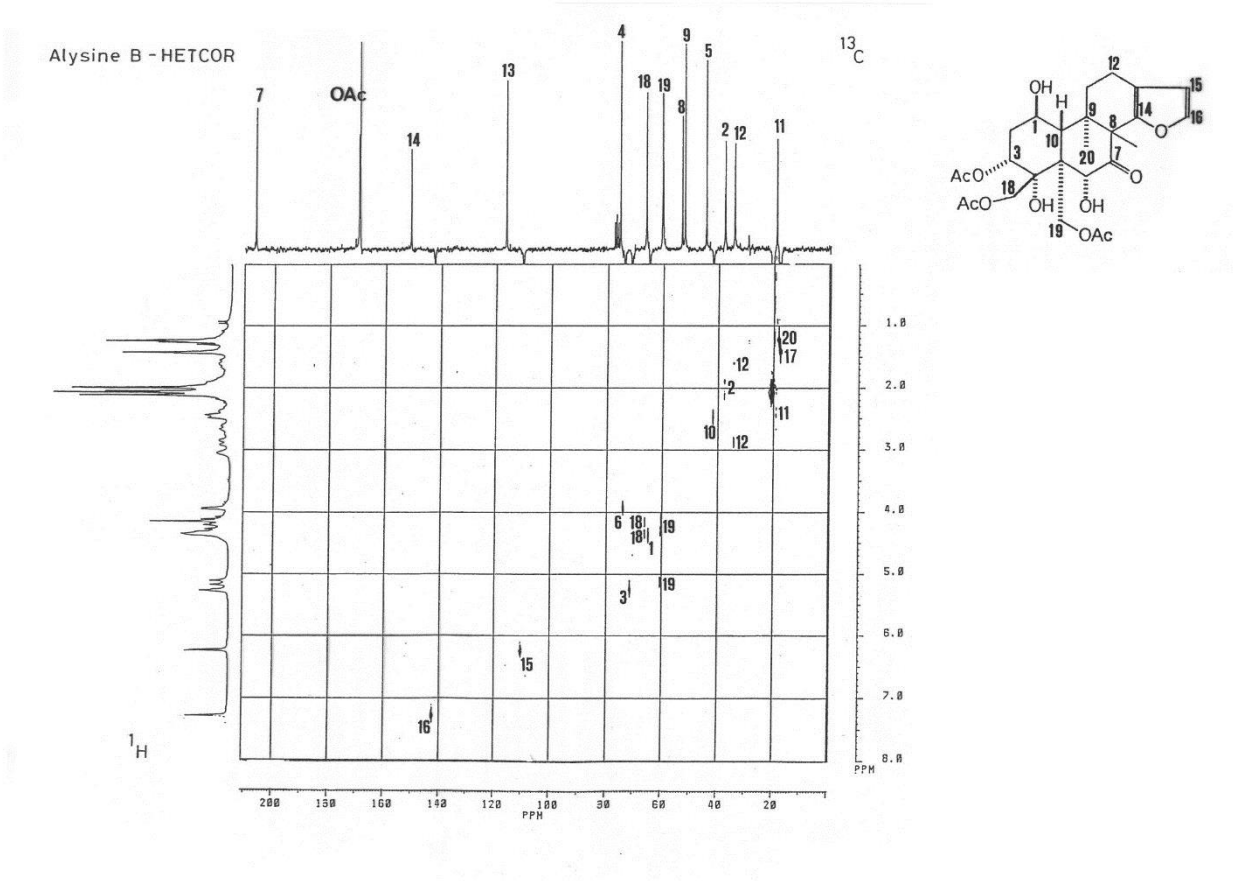


**Figure S8.** $^{1}H$–$^{13}C$ correlation (HETCOR) spectrum of alysine B.

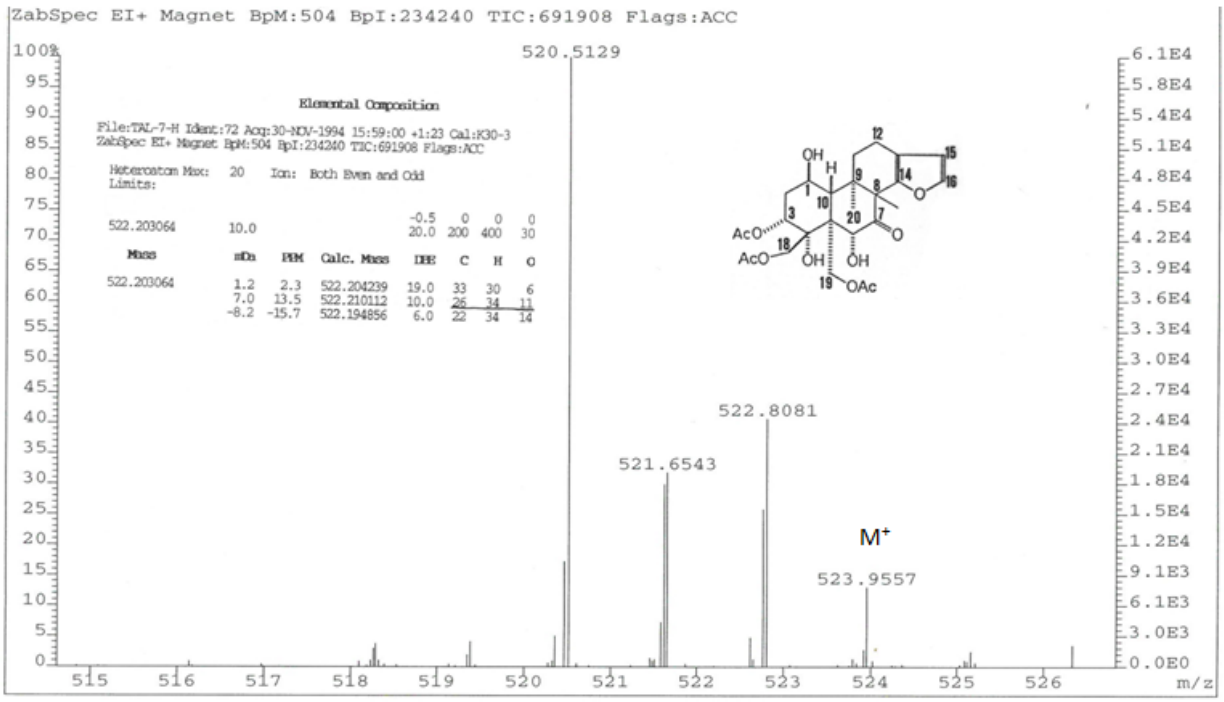


**Figure S9.** HRMS (EI) spectrum of alysine B.

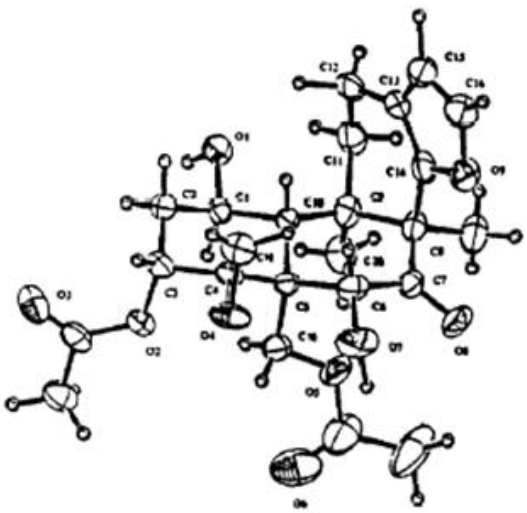

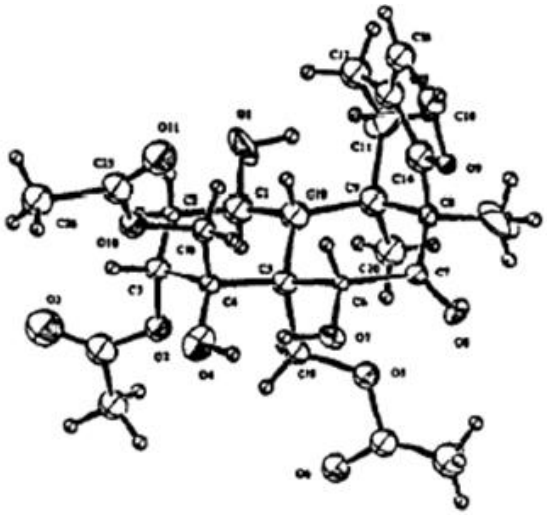

| Compound | 1 | 2 |
|---|---|---|
| Formula | $C_{24}H_{30}O_9$ | $C_{26}H_{34}O_{11}$ |
| fw | 462.50 | 522.55 |
| crys. syst. | orthorombic | monoclinic |
| space group | $P2_12_12_1$ | $P2_1$ |
| crys. dimens., mm | 0.20 x 0.20 x 0.30 | 0.15 x 0.02 x 0.30 |
| a, A° | 15.505 (7) | 8.901 82) |
| b, A° | 15.902 (4) | 13.228 (2) |
| c, A° | 9.360 (3) | 11.156 (3) |
| ß (°) | - | 101.4 (2) |
| z | 4 | 2 |
| V, A° | 2308 (2) | 1287.8 (6) |
| D (calcd.) g $cm^{-3}$ | 1.331 | 1.347 |
| radiation | CuKα | CuKα |
| abs. coeff (μ), cm-1 | 8.10 | 8.44 |
| F(000), e | 984 | 556 |
| temp, °C | 23 | 23 |
| diffractometer | Rigaku AFC6S | Rigaku AFC6S |
| scan mode | ω-2θ | ω-2θ |
| $2\theta_{max}$ | 158.0° | 157.8° |
| total data collected | 4752 | 5324 |
| unique data | 2711 | 2796 |
| observed data used | 3023 [I>3σ(I)] | 2106 [I>3σ(I)] |
| no. of params. refined | 383 | 179 |
| max shift/error on final cycle | 0.05 | 0.18 |
| max. resid. density, e /A°3 | 0.21 | 1.35 |
| R, Rw | 0.055; 0.047 | 0.178; 0.136 |
| GOF = $[\Sigma w(\|Fo\|-\|Fc\|)^2/(No-Nv)]^{1/2}$ | 2.73 | 4.53 |

**Figure S10.** X-ray spectra, crystal data, and data collection and refinement parameters of alysine A and alysine B.